Future Dutch Electricity Grid: Assessing the Potential of Overplanting in Photovoltaic Systems

Francisco Reis
Delft University of Technology
Delft, Netherlands
reis.fran@hotmail.com

José Rueda Torres, Peter Palensky
Delft University of Technology
Delft, Netherlands
J.L.RuedaTorres@tudelft.nl

Francisco Gonzalez-Longatt
DIgEnSysLab, University of Exeter
Exeter, United Kingdom
fglongatt@fglongatt.org

***Abstract*—This paper concerns with the determination of a suitable level of overplanting for photovoltaic systems. For this purpose, six futuristic operational scenarios for the Dutch electrical power system are generated for year 2050. A synthetic model is developed by using DIgSILENT Power Factory 2022 SP3 to investigate the steady-state systemic performance in each operational scenario, taking into account three cases with different levels of overplanting. Power flow calculations are conducted to reflect on the resulting voltage profiles and active power losses as well as on the implications on the required network upgrades (e.g. addition of lines, transformers, and reactive power compensation devices).**

***Keywords*—power system, national scenario, overplanting, photovoltaic systems, power flow**

I. Introduction

The European Union and the Dutch government currently pursue an accelerated energy transition to achieve climate neutrality related milestones by year 2050. This urgently requires a thorough investigation of possible technological upgrades and their impact on the national electrical power system. Such investigation shall also take into account a high degree of uncertainty, due to different factors like variable generation and demand profiles and the reliability of emerging technologies for power electronic interfaced generation, transmission, distribution, compensation, and consumption. This paper focuses on defining the most advantageous level of overplanting in photovoltaic (PV) systems, taking as example synthetic operational scenarios generated based on publicly available projections for the electrical power system in the Netherlands by year 2050.

The idea is to install a PV system, whose connection capacity is only a fraction of the rated power of the solar panels. The goal is to decrease the peak in the feed-in profile of the PV system, effectively making it "flatter". This aspect reduces the variability of solar power, which helps keeping the grid balanced. According to [1], the Dutch grid operators and solar PV industry agreed that large PV systems built after the end of 2020 could be allowed to have a connection capacity of up to 70% of the rated power from the solar panels. Besides, it is also estimated that in the future this limit may be decreased to 50%. Given the large installed capacity of solar PV systems expected for 2050, this uncertainty can generate significant changes in the necessary grid investments. The scenarios defined for the future Dutch power system in [2] and [3] do not take this aspect into consideration. In [4] and [5], overplanting in PV systems is acknowledged but not studied. Instead, connection capacity is still considered to be the same as solar panel installed capacity, with the later being decreased. In addition, the efficiency of the PV systems is assumed to increase up to 40%. Lastly, [1] considers a hypothetical connection capacity of solar PV systems to be 66% of the installed solar panel capacity.

For the targeted investigation, a synthetic model of the Dutch electricity grid is created in DIgSILENT PowerFactory 2022 SP3 and a scenario for 2050 is implemented with three different levels of overplanting, 50%, 60% and 70%, respectively. In order to evaluate the performance of the three settings, six operational scenarios are considered. A power flow is executed for every case in each operational scenario and the results are compared and discussed.

This paper is organized in the following manner, Section II presents the scenario created for the Dutch power system in 2050. Section III describes the development of the synthetic model in DIgSILENT Power Factory 2022 SP3. Section IV introduces the sensitivity analysis based on power flow calculations, explains the evaluation metrics, and shows the results. Finally, Section V presents the general conclusions.

II. Defining the Scenario for the 2050 Power System

The method utilized to create a scenario of the Dutch power system in 2050 is presented as a flowchart in Fig. 1.

A. Analysis of Future Scenarios and Current Strategy

In [1], [2], [4] and [5], the Regional and the National scenarios aim for energy independence and self-sufficiency, with the Regional scenario focusing on a high level of autonomy and the power supply is dominated by decentralized PV systems, while the Nacional scenario gives control to the

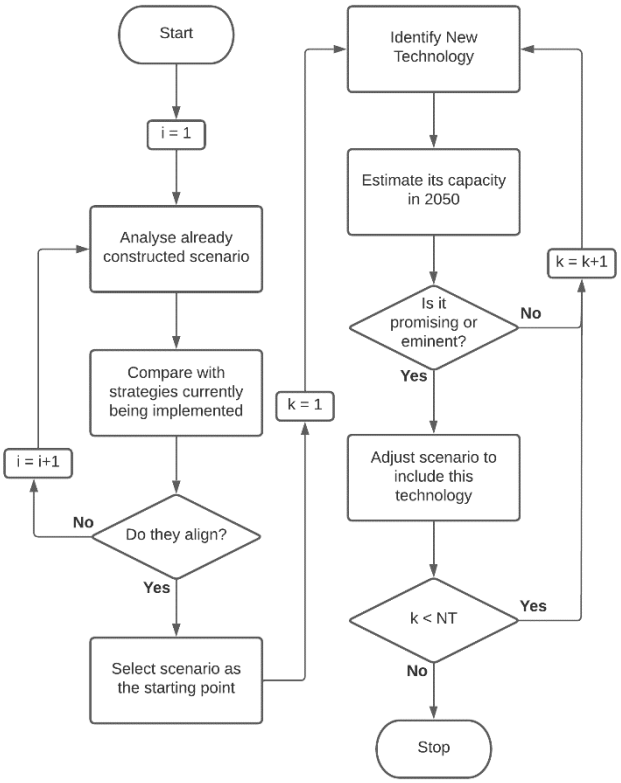

Fig. 1. Definition of the scenario for the Dutch power system in 2050.

national government and the main focus is offshore wind power. In the European and/or International scenario, international energy exchange is prioritized, trying to find the most cost-effective options. The most recent versions of these scenarios are presented in [1]. In [3], the main focus is on the scale of investment in variable renewable energy sources (VRES) and in the share of energy demand allocated to gas in the future. The goal is to understand how much renewable electricity should be generated in the Netherlands and if it should be directly used or further converted with power-to-gas technologies.

A strong ambition for offshore wind power is shown in [6], aiming for an installed capacity over 50GW in 2050. A large part of the electricity generated from offshore wind will be used for hydrogen production, as the Netherlands strive to be in the centre of hydrogen production and trading in Europe [7]. Therefore , the National scenario from [1] is chosen.

B. *Adjustments Made to the Selected Scenario*

In Fig. 1, *NT* represents the number of technologies analysed. It is stated that there is the potential to have installed around 10GW of floating solar panels in between the wind turbines in [8]. So, 10GW of the total capacity of installed solar fields was considered to be offshore. Recently, plans were announced to build two new nuclear power plants in Borselle [9], having a combined installed capacity of around 3GW, which were subtracted from the installed capacity of large gas power plants and allocated to nuclear power. Lastly, the potential capacity of demand response was defined. The first one is industrial demand side response whose potential was estimated in [10] for 2020 and in [11] for 2030 and, considering the growth in that decade, it was assumed 5.2GW of capacity for this option in 2050. The second option is the use of heat pumps in the built environment, whose capacity of 7GW was defined in [11]. Electric boilers for industry are the last option for demand response, corresponding to 4GW, estimated in [11]. Table I presents an overview of the scenario created for the Dutch power system in 2050.

TABLE I. MIX OF SUPPLY, DEMAND AND FLEXIBILITY IN 2050

Supply [GW]	**212.5**
Solar Power	**106.5**
Onshore (Roofs + Fields)	96.5
Offshore	10
Wind Power	**71.5**
Onshore	20
Offshore	51.5
H_2 Power Plant	**31.5**
Large Unit	19
Small Unit	12.5
Nuclear Power Plant	**3**
Peak Demand [GW]	**40**
Households	7
Services	5
Industry	18
Transport	5
Agriculture	4
Other	1
Flexibility [GW]	**120.2**
Electrolyser	**50.6**
Battery Storage	**53.4**
Centralized	26.7
Decentralized	26.7
Demand Response	**16.2**
Industrial Demand Side Response	5.2
Heat Pumps for Built Environment	7
Electric Boilers for Industrial Heat	4

III. DEVELOPMENT OF THE SYNTHETIC MODEL FOR 2050

The model presented in this section was developed in DIgSILENT PowerFactory 2022 SP3. Fig. 2 displays the single line diagram of the synthetic model developed, separated in geographical zones.

A. *Description of the Base Model*

This model of the Dutch high voltage grid for 2050 was built from the synthetic model for 2030 developed in [12]. The grid was built using single line diagrams from [13] and [14] and its expansion followed ongoing or planned projects listed in [15].

Regarding the modelling of system components, the busbars are developed as simple terminals (*.ElmTerm) operating at nominal voltage. The 27 synchronous generators (*.ElmSym) installed share the same parameters (except rated capacity) and operate at 15kV. Solar PVs and wind turbines are modelled as static generators (*.ElmGenstat) and are directly connected to the high voltage busbars. In each region, one PV system and one onshore wind turbine are installed in the 110/150kV busbar and represent the accumulated installed capacity of that technology inside the region in question. Offshore wind turbines are connected to the 220/380kV busbars. To aid in voltage regulation, generators representing PV systems and offshore wind turbines were considered to have the ability to work as static synchronous compensators

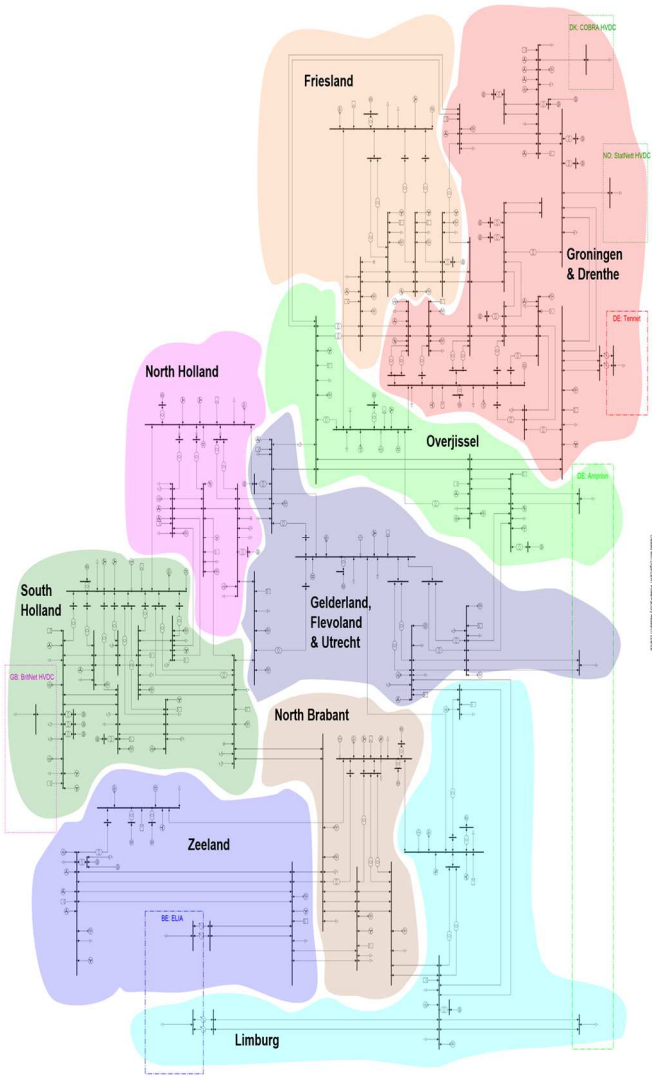

Fig. 2. Division of the single line diagram into geographical zones.

(STATCOMs). The loads are modelled as general load type (*.ElmLod) with no voltage dependency and are implemented in the same way as PV systems and onshore wind turbines. Transmission lines (*.ElmLne) were modelled according to the data provided in [13]. For new transmission lines, values were used for typical 400 kV 50HZ overhead lines [16]. All the transformers used are modelled as a two-winding transformer type (*.ElmTr2). Interconnections and electrolysers are represented as loads.

B. Modifications Made to the Base Model

Research was made with the purpose of listing already planned network expansions. The only one found that isn't already implemented in the base model is a new 380kV connection between Ens and Vieverlaten [17]. Two parallel transmission lines with a length of 90km were implemented in the model, using the line type defined for new transmission lines in the base model. Further changes in the transmission lines and transformers are dependent on the results from the simulations, Section IV exposes this process in greater detail.

All of the new grid components introduced in the synthetic model were implemented, following the methodology used in the base model. In order to achieve more realistic power flows, part of the onshore wind power, solar power and demand was distributed across the busbars in the 220/380kV network. One municipality was attributed to each busbar. Then, data related to wind and solar power installed capacity and demand in each municipality was extracted from [18] and scaled up to meet the 2050 values. A battery was also installed in each of these busbars as a static generator (*.ElmGenstat) and their capacity is related to the number of homes and electric cars in the respective municipality [18]. One electrolyser was installed in each province and the installed capacity is proportional to the VRES installed capacity in that province. Finally, gas power plants were considered as hydrogen power plants and coal power plants were disconnected.

IV. Sensitivity Analysis

To determine the most beneficial level of overplanting, a sensitivity analysis was conducted, comparing the results for three different cases. In case A the grid connection capacity for PV systems is 50% of the solar panel installed capacity, in case B it is 60% and in case C it is 70%. The analysis consists of testing the three cases under six operational scenarios (OS):

- o OS1: Rated solar and wind power infeed
- o OS2: Rated solar power infeed
- o OS3: Rated wind power infeed
- o OS4: Rated conventional generation
- o OS5: Average Summer day
- o OS6: Average Winter day

Fig. 3 presents a flowchart, describing how cases A, B and C are tested under each operational scenario. Nuclear power is dispatched in every scenario close to nominal conditions. Peak demand is considered in the first four operational scenarios, while 30GW of demand are assumed in the last two.

When performing power flow calculations in DIgSILENT PowerFactory 2022 SP3, the power flow equations used are based on the nodal admittance (Y-bus) matrix formulation. Therefore, the power flow equations, representing the active power and reactive power balance for each bus *i* in the system,

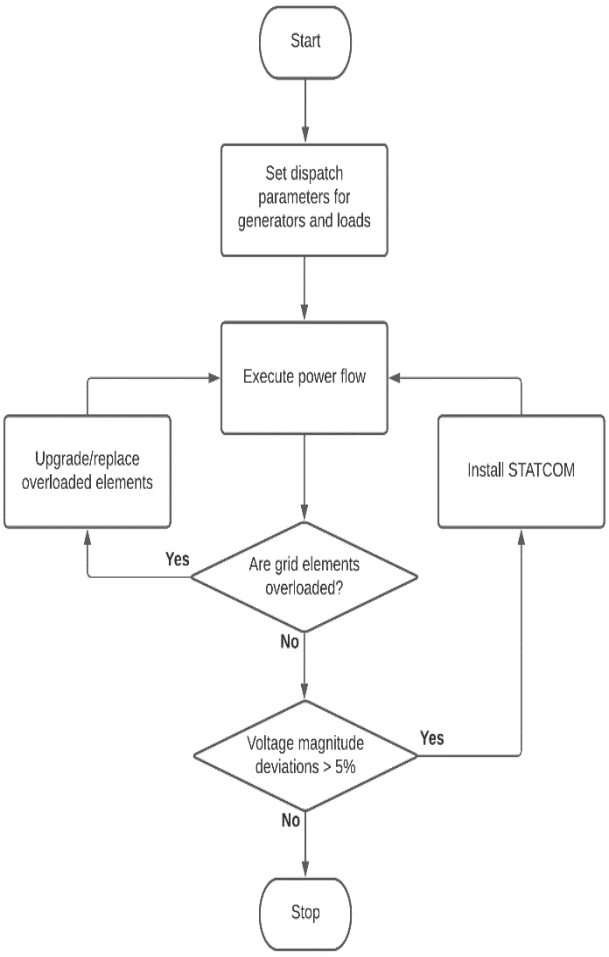

Fig. 3. Method used to test the three cases under each operational scenario.

are shown in (1) and (2), respectively.

$$P_i = \sum U_i U_j Y_{ij} cos(\delta_i - \delta_j - \theta_{ij}) \quad (1)$$

$$Q_i = \sum U_i U_j Y_{ij} sin(\delta_i - \delta_j - \theta_{ij}) \quad (2)$$

In (1) and (2), P_i is the active power injection at bus i, Q_i is the reactive power injection at bus i, U_i is the voltage magnitude at bus i, U_j is the voltage magnitude at bus j, Y_{ij} is the admittance of the transmission line between buses i and j, δ_i is the voltage phase angle at bus i, δ_j is the voltage phase angle at bus j and θ_{ij} is the admittance phase angle of the transmission line between buses i and j.

A. Installed Transmission Lines and Transformers

As the PV systems connection capacity increases from case A to case C, more investment will be needed in grid elements to deal with the increasing amounts of power flowing through the network. Fig. 4 and Fig. 5 present this increase in required transmission line and transformer installed capacities, respectively. It is clear that, from case A to case B and from case B to case C, the increase in installed connection capacity for PV systems is the same, but the increase in transmission lines and transformers capacity is not. Upgrades made to the transmission lines in case A represent 19% of the total transmission line capacity installed in the base case, while for case B this value is around 25%. So, the additional investment is equivalent to 6%. In contrast, the necessary upgrade in case C corresponds to 48% of the transmission lines capacity in the base model. This means that the change from case B to case C requires adding an extra 23%

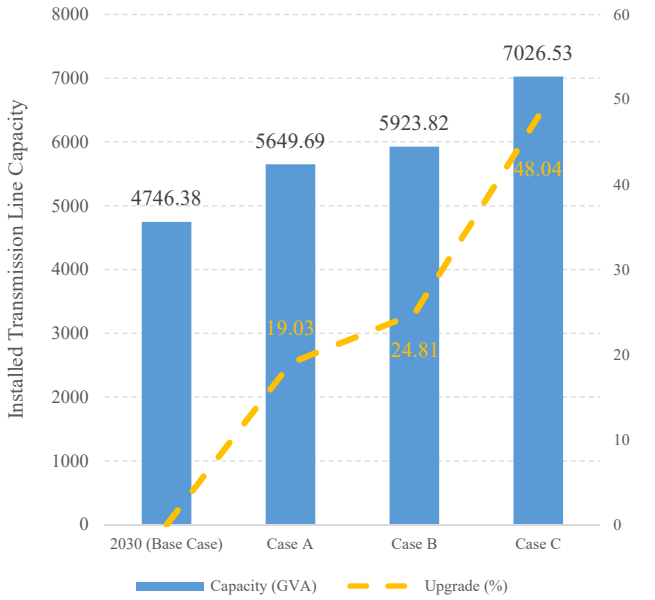

Fig. 4. Change in installed transmission line capacity from the base case to cases A, B and C.

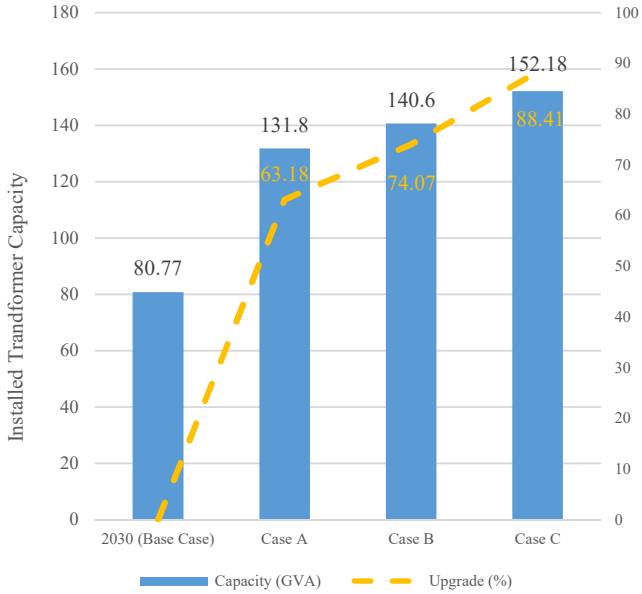

Fig. 5. Change in installed transformer capacity from the base case to cases A, B and C.

and the same situation occurs when it comes to the transformers, although not as noticeable. From case A to case B, the added investment corresponds to 11% of the total transformer capacity in the base model, while from case B to case C, this difference increases to 14%. These results indicate that the trade-off between added installed PV system connection and additional grid investments is substantially worse when case C is implemented.

B. Reactive Power Compensation

In every operational scenario, reactive power compensation devices (STATCOMs) were installed to guarantee that the deviations in busbar voltage magnitudes were under 5%. In Fig. 6, the location where the STATCOMs are installed is presented and Fig. 7 shows the reactive power compensation required in each operational scenario. Case C presents the biggest need for reactive power compensation

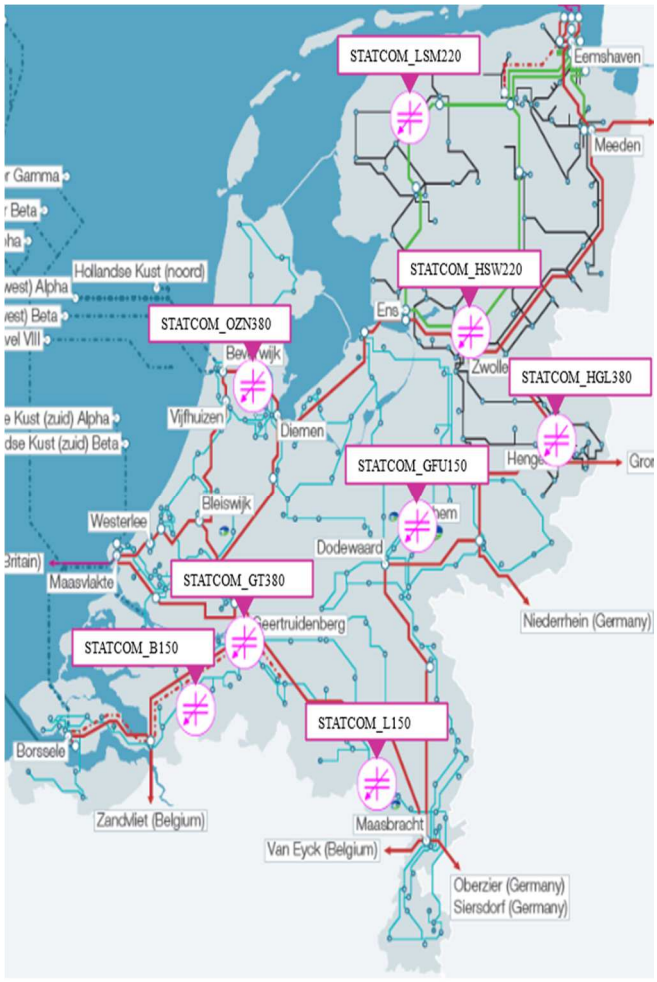

Fig. 6. Grid map from [19], highlighting the location of the STATCOMs.

and, consequently, the largest number of devices, mostly due to OS1. Here, the extreme amount of power supplied is met by deploying all electrolyser and battery capacity, plus some demand response, which decreases the voltage magnitude in many busbars across the grid. In OS3 and OS6, where the power supply is the same in all cases, the difference in required reactive power depends only on the grid elements. Fig. 4 and Fig. 5 show that the investments in transmission lines and transformers increase from case A to case C. Hence, case A displays the biggest need for reactive power compensation in these scenarios, followed by case B and then case C. Lastly, in OS2 and OS5, case B clearly performs better than the other cases, needing much less reactive power compensation. The similarity between these scenarios is the supply being dominated by solar power. As solar power is much more decentralized than wind power, this signs a good balance between local supply and demand for the PV system connection capacity considered in case B.

C. Active Power Losses

In certain operational scenarios, active power supply varies from case to case, so, to ensure a fair comparison, the ration between active power losses and active power supplied is considered and presented in Fig. 8. OS1 and OS5 present a similar trend, as the infeed of solar power increases, so does the percentage of dissipated active power. This stems from the fact that, as supply increases, local flexibility options reach their maximum capacity and the surplus is transferred to other regions of the grid, where more storage units are available.

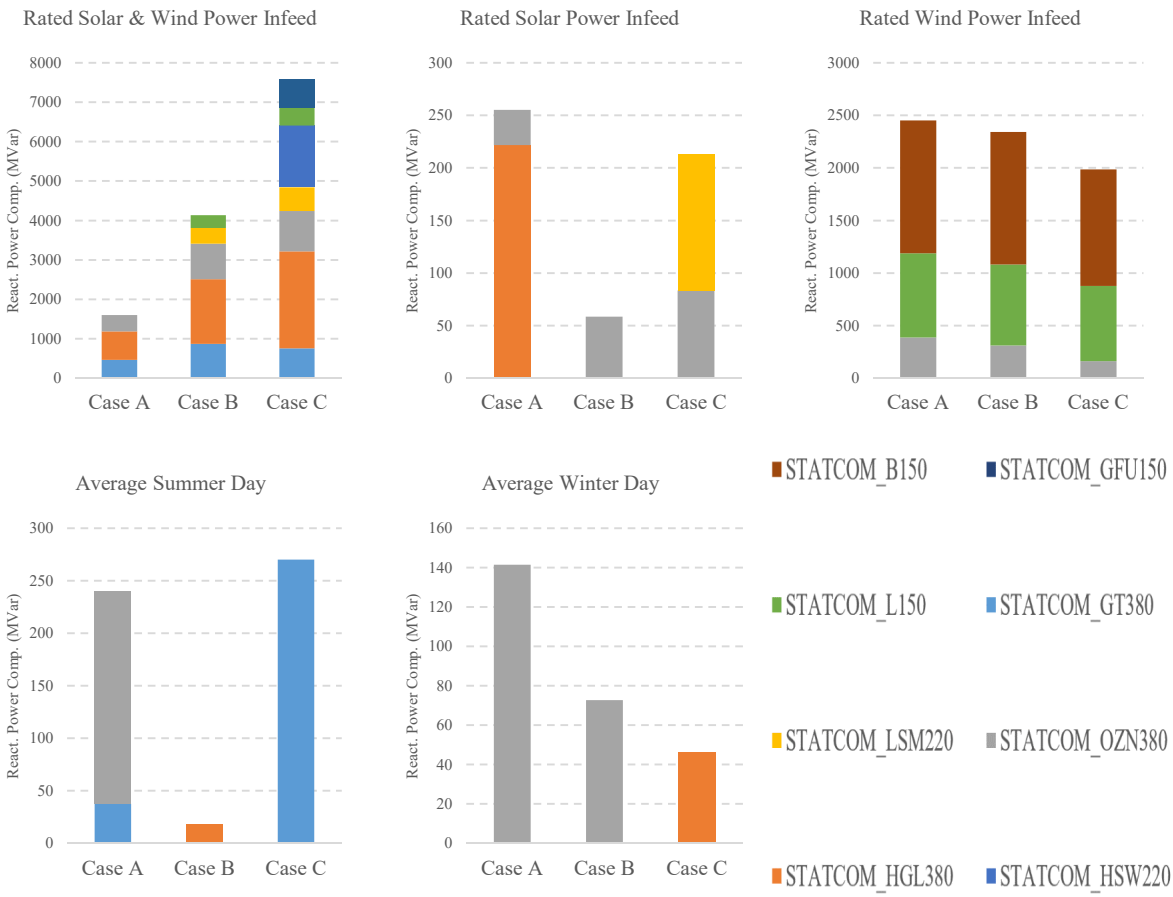

Fig. 7. Installed STATCOMs and respective compensation in each operational scenario (in absolute values)

This increase in power flows leads to the loss of a bigger share of the active power supplied in transmission lines and transformers. Thus, case C presents the biggest percentage of wasted active power, followed by case B and then case A. OS2 does not follow this trend due to case B, which presents better results than case A, even with a larger infeed of solar power. Again, this happens due to the local balance between supply and demand in case B. Contrarily, in case A the demand in certain regions is not met by the local supply and in case C the local supply is not met by the demand and flexibility options of that region, generating more power flows. As it was explained in the previous topic, the correlation between grid performance and grid investments is highlighted in the operational scenarios where the power supplied is the same for the three cases. Therefore, in OS3, OS4 and OS6, case A, where the smallest investments in transmission lines and transformers were made, registers the highest active power losses.

D. Busbar Voltage Magnitudes

Since the first four operational scenarios present extreme situations, here is where the biggest voltage magnitude deviations occur. Even so, in OS4, this is mitigated by the fact that the synchronous generators contribute to voltage regulation and batteries are also dispatched in busbars with low voltage magnitudes. Fig. 9 displays the results for the voltage magnitudes in OS1, OS2 and OS3 in the form of heat maps. In OS1, it is possible to see that voltage magnitudes decrease in many busbars as the PV systems connection capacity increases. With the increase in solar power infeed, the need for flexibility options increases and spreads to other busbars where there is still available capacity, thus the

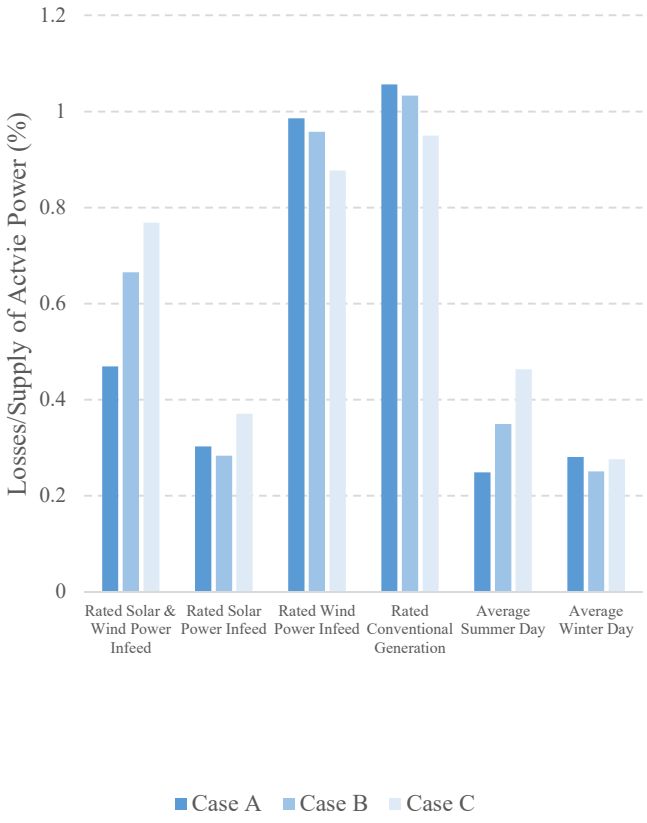

Fig. 8. Percentage of active power dissipated in each operational scenario.

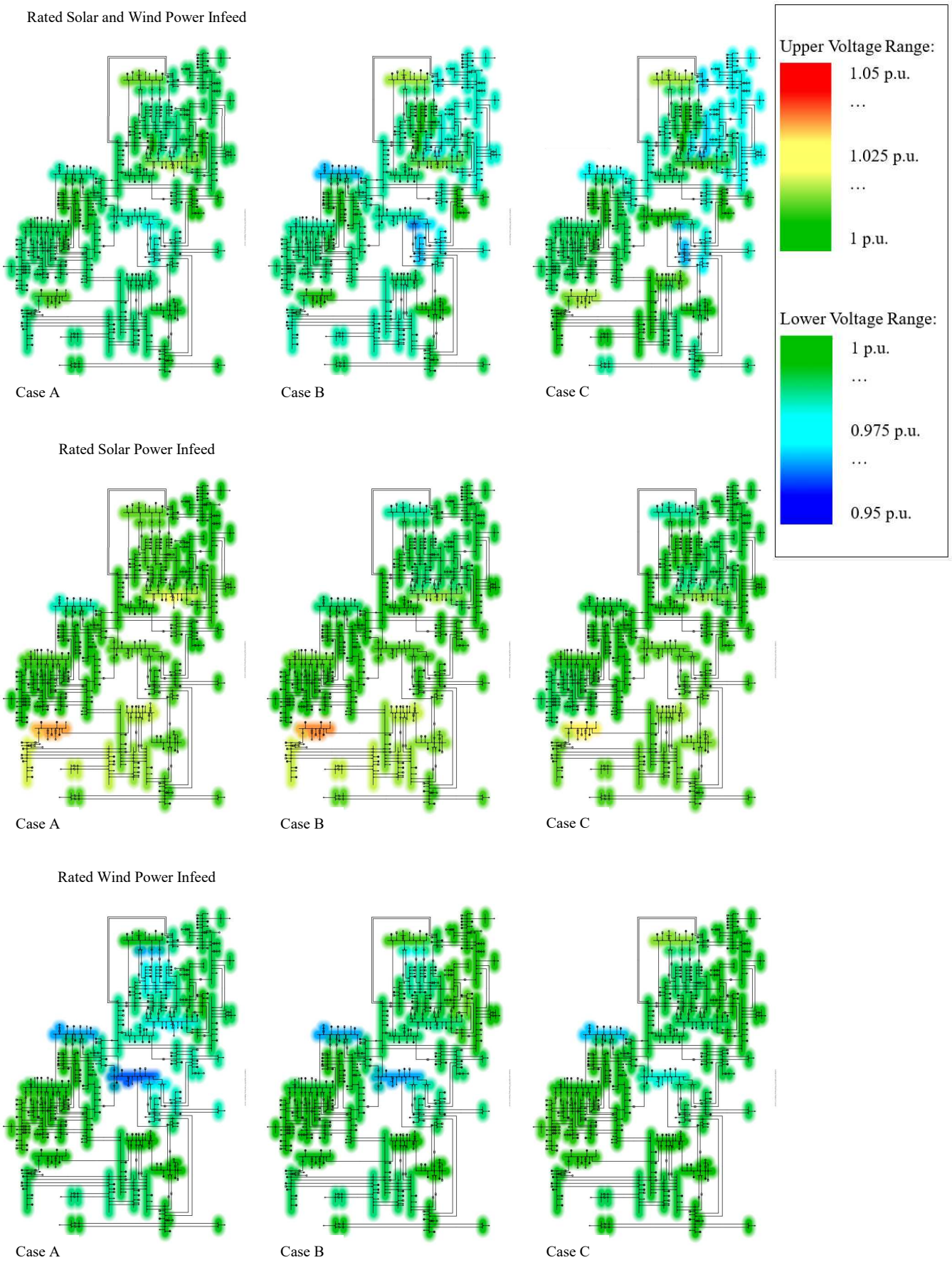

Fig. 9. Comparison of busbar voltage magnitudes between the three cases in OS1 (top), OS2 (middle) and OS3 (bottom).

difference in voltage magnitudes from case A to case B and case C. In OS2, the main issue occurs in the region of Zeeland, where there is a clear over voltage. In contract, OS3 displays under voltage problems in the 150kV networks of North Holland and of the combined region of Gelderland, Flevoland and Utrecht, as the significant number of battery units in these provinces store a large part of the surplus from offshore wind power. However, these problems are less prominent from case A to case B and even less so from case B to case C, due to the large increase in grid investments which make the network more robust. In the remaining operational scenarios, all cases performed well, with small deviations in busbar voltage magnitudes.

E. Overview of the Sensitivity Analysis

Summarizing the results, case C performed well, displaying voltage magnitudes close to optimum and low active power losses in the operational scenarios where the supply was the same across the three cases. Nevertheless, the difference to the other two cases was not significant enough to justify the excessive investment in reactive power compensation devices, transmission lines and transformers. The remaining cases had similar results when it comes to busbar voltage magnitudes, excluding OS1, where case B suffered from under voltage in certain regions of the network, due to extensive use of batteries and electrolysers. In contrast, case B required less reactive power compensation and had a smaller percentage of dissipated active power in most of the operational scenarios.

Besides, in the base model, solar PV systems are designed to work as STATCOMs, enabling them to contribute to voltage control. This concept is further explored and tested in [20], demonstrating that PV systems can utilize their remaining capacity for reactive power injection or absorption when injecting active power into the grid. In scenarios without solar radiation, the entire connection capacity can be utilized for voltage regulation, and during emergencies, the PV system can temporarily cease active power generation to allocate the full capacity for voltage control. This adds value to having additional connection capacity for PV systems, offering extra capacity for voltage control in every busbar. Taking this factor into account, the analysis concludes that case B is the most advantageous configuration for the 2050 model of the Dutch electricity grid.

V. Conclusion

The synthetic model from [12] served as the base, which was worked on and rearranged to represent what the Dutch grid may look like in 2050. From the estimated scenarios for 2050, the National scenario from [1] was adopted and adjusted according to other publicly available data. The distribution of the supply, demand and flexibility options across the provinces and then across the busbars inside each province was also considered in the calculated power flows.

The main factor to be defined was the overplanting in PV systems. The feasible range for the installed connection capacity is between 50% and 70% of the total solar panel capacity. So, after performing a sensitivity analysis, case B, which considered the connection capacity to be 60% of the installed solar panel capacity, displayed the best compromise between grid performance and required investments. Coupling these results with the added advantage of having extra connection capacity available for voltage regulation (if solar PV systems are considered to work as STATCOMs), lead to the conclusion that case B is the most beneficial option. Additional research efforts are being devoted to the addition of primary control systems and the study of their impact on the stability-related operational boundaries.

References

[1] Netbeheer Nederland, “Het energiesysteem van de toekomst”, Apr. 2021,URL:https://www.netbeheernederland.nl/_upload/Files/Samenvatting_rapport_Het_Energiesysteem_van_de_toekomst_198.pdf.

[2] CEDelft, “Net voor de toekomst”, Nov. 2017, URL: https://www.ce.nl/publicaties/2030/netvoor-de-toekomst.

[3] TenneT and Gasunie, “Phase II — pathways to 2050”, Apr. 2021, URL: https://www.tennet.eu/company/publications/ii3050/.

[4] Berenschot, “Nederland klimaatneutraal in 2050: vier scenario’s”, Apr.2020,URL:https://www.berenschot.nl/media/hl4dygfq/rapport_klimaatneutrale_energiescenario_s_2050_2.pdf.

[5] TenneT and Gasunie, “Infrastructure outlook 2050”, Feb. 2020, URL: https://www.tennet.eu/infrastructure-outlook-2050.

[6] Dutch Ministry of Economic Affairs and Climate, “Letter to parliament on offshore wind energy 2030-2050”, Sep. 2022, URL: https://english.rvo.nl/sites/default/files/2022/10/Letter-to-Parliament-Offshore-Wind-Energy-2030-2050.pdf.

[7] RVO, FME, Topsector Energie and TKI New Gas, “Excelling in hydrogen: Dutch technology for a climate-neutral world”, Apr. 2023, URL: https://www.fme.nl/hydrogen-guide-2023.

[8] DNV GL, “North sea energy outlook”, Nov. 2020, URL: https://www.government.nl/documents/reports/2020/09/01/report-north-sea-energy-outlook.

[9] People’s Party for Freedom and Democracy, Christian Democratic Alliance, Democrats ’66 and Christian Union, “2021-2025 Coalition agreement”,Dec.2021,URL:government.nl/documents/publications/2022/01/10/2021-2025-coalition-agreement.

[10] TenneT, “Unlocking industrial demand side response”, July 2021, URL:https://netztransparenz.tennet.eu/fileadmin/user_upload/Company/News/Dutch/2021/Unlocking_industrial_Demand_Side_Response.pdf.

[11] Aurora Energy Research, “CO_2-free flexibility options for the Dutch power system”, Oct. 2021, URL: https://auroraer.com/insight/co2-free-flexibility-options-for-the-dutch-power-system/.

[12] Anouk de Roos, “Synthetic steady-state model of the 2030 Dutch EHV network”, June 2021, unpublished.

[13] TenneT, System & transmission data Explanatory Documents Griddiagram,2019,URL:https://www.tennet.org/english/operational_management/transmission_services/Calculated_crossborder_cap/explanatory_documents.aspx.

[14] Hoogspanningsnet.com, Netkaart van Nederland, 2021, URL: https://www.hoogspanningsnet.com/netschema/.

[15] TenneT, “Investeringsplannen, net op land 20202029”, Tech. rep. TenneT,Oct.2020,URL:https://www.tennet.eu/nl/bedrijf/publicaties/investeringsplannen/.

[16] Hossein Khalilnezhad et al. “Influence of long EHV AC underground cables on the resonance behavior of the Dutch transmission system”. In: 2016 IEEE Power and Energy Society General Meeting (PESGM). IEEE. 2016, pp. 1–5, in press.

[17] TenneT, “Vierverlaten - Ens 380 kV”, 2023, URL: https://www.tennet.eu/nl/projecten/vierverlaten-ens-380-kv.

[18] Rijksoverheid, De Regionale klimaatmonitor, 2022, URL: https://klimaatmonitor.databank.nl/jive.

[19] TenneT, Grid Map Onshore Netherlands, 2023, URL: https://www.tennet.eu/grid/grid-maps.

[20] Rajiv K. Varma and Ehsan M. Siavashi, “PV-STATCOM: a new smart inverter for voltage control in distribution systems”, in: IEEE Transactions on Sustainable Energy, Oct. 2018, pp. 1681-1691, in press.